Escalating Hydroclimatic Extremes and Volatility in the UK Under 2 °C and 4 °C Warming

Y. He[1], D. Manful[1], N. Forstenhäusler[1], Y. Huang[2], B. Smith[3], and Q. Zha[1]

[1] Tyndall Centre for Climate Change Research, School of Environmental Sciences, University of East Anglia, UK.

[2] College of Civil Engineering, Fuzhou University, Fuzhou 350108, China.

[3] School of Engineering, Newcastle University, UK.

Corresponding author: Yi He (yi.he@uea.ac.uk)

Key Points:

- Future warming will increase both floods and droughts across different parts of the United Kingdom
- Sudden shifts between dry and wet conditions will become more common, creating new challenges for water planning
- This study provides one of the most comprehensive UK national-scale assessments of river flow changes under climate warming

Abstract

Hydrological extremes, including both floods and droughts, are projected to intensify under global warming, yet their joint evolution and variability across temperate catchments remain underexplored. This study uses bias-corrected regional climate projections from the UK Climate Projections 2018 (UKCP18) and a distributed HBV-TYN hydrological model to simulate future river flows across 698 UK catchments under 2 °C and 4 °C global warming scenarios. Compared to previous UK-wide assessments, this study provides the most extensive high-resolution, bias-corrected, ensemble-based analysis of river flow responses under warming-level-specific timeframes. A comprehensive suite of hydrometeorological metrics is applied, including the maximum number of consecutive dry days, extreme precipitation totals, high and low flow percentiles, flood return levels, and the Standardised Precipitation and Streamflow Indices. Results reveal a regionally divergent intensification of extremes of extremes: (1) precipitation extremes intensify under warming, with daily and multi-day rainfall maxima increasing in western and northern regions, while dry spells lengthen in the south and east; and (2) high flows and flood magnitudes increase especially in western and northern regions, while persistent low flows and drought frequency intensify in the south and east. Projections also indicate a growing incidence of hydroclimatic whiplash, abrupt shifts between wet and dry extremes, posing challenges for water resources management. This is the first national-scale UK study to quantify hydrological whiplash across a full climate ensemble. These findings highlight the urgent need for regionally tailored, climate-resilient water management strategies to address the compounding risks of flooding, drought, and increased hydroclimatic volatility under future warming.

Plain Language Summary

Climate change is expected to increase both floods and droughts in many regions, but understanding how these changes will play out locally is crucial for managing water resources and preparing for future risks. In this study, we analysed how river flows across the United Kingdom (UK) might change as global temperatures rise by 2 °C and 4 °C. We used climate projections and a national hydrological model to simulate changes in rainfall, streamflow, and extremes in 698 river catchments across the UK. Our results show that flood events are likely to become more intense in the western and northern UK, while long dry periods and low river flows will worsen in the south and east. We also found that sudden shifts between wet and dry conditions which is known as hydroclimatic whiplash are expected to become more frequent. These changes could make it harder for water managers to plan for droughts or floods, especially in regions that face both risks. Our findings can help inform region-specific strategies to adapt to climate change and improve the resilience of water systems. The UK provides an important example of how global warming could affect river systems in other temperate climates around the world.

1 Introduction

Climate change is intensifying the global water cycle, leading to greater variability in river flows and altering the frequency and severity of both floods and droughts (Arnell and Gosling, 2016; Müller et al., 2024). These shifts have far-reaching consequences for water supply, water quality, ecosystem health, and energy production. Understanding how hydrological extremes

evolve under different global warming levels is essential for designing resilient water management and climate adaptation strategies.

In the United Kingdom (UK), several studies have explored how climate change may affect streamflow and water availability. The UK Climate Projections 2009 (UKCP09) and its successor, the UK Climate Projections 2018 (UKCP18), have played a central role in supporting this research. Among the four UKCP18 strands, the 12-member regional climate model (RCM) ensemble provides high-resolution projections (12 km) tailored for impact studies, especially at the catchment scale. This dataset has supported a wide range of hydrological impact assessments, including projections of river and groundwater flows (Kay, 2021; Hannaford et al., 2023; Smith et al., 2024), flood and drought extremes (Griffin et al., 2022; Reyniers et al., 2023), and multi-sectoral water risk analysis (Arnell et al., 2021).

Key findings from these studies indicate complex spatial patterns in projected flow changes. For example, Kay (2021) used the national-scale Grid-to-Grid (G2G) model to project substantial summer flow reductions, particularly in southern and eastern regions, alongside winter flow increases. Arnell et al. (2021) found increased flood risks in western parts of the UK but limited changes in the southeast, and widespread increases in drought frequency. Lane et al. (2022), using the DECIPHeR model, identified substantial increases in high flows in western regions but a general decline in median flows in Great Britain. Griffin et al. (2022) noted intensifying winter flood events in the future (2051-2080), though their projections did not apply bias correction to the climate data. Reyniers et al. (2023) highlighted a significant rise in meteorological drought indicators across Great Britain, particularly under high-emissions scenarios. Smith et al. (2024), using the SHETRAN model, reported strong declines in flows in the south and east but highlighted regional increases in high-flow extremes in the north and west.

Despite these advances, key gaps remain. Many existing studies focus only on Great Britain, omit Northern Ireland, or lack bias correction of RCM data, which is crucial for accurately representing precipitation extremes (Fung, 2018; Teutschbein and Seibert, 2013). Furthermore, few studies adopt a warming-level framework aligned with international climate targets, and even fewer address the growing concern of hydroclimatic whiplash, sudden shifts between wet and dry conditions.

This study addresses existing gaps by providing a comprehensive, bias-corrected, ensemble-based assessment of river flow changes across 698 UK catchments, spanning all devolved nations. We use daily, bias-corrected outputs from all 12 UKCP18 regional climate model ensemble members to drive a distributed hydrological model (HBV-TYN), and evaluate impacts at 2 °C and 4 °C above pre-industrial temperatures. A wide range of hydrometeorological and hydrological indicators is used to assess drought and flood hazards, including extreme precipitation, flow percentiles, return-level floods, and the Standardised Precipitation Index and Standardised Streamflow Index. For the first time for the UK, we also quantify changes in hydrological whiplash based on streamflow shifts from dry to wet and wet to dry conditions. These analyses aim to improve understanding of how warming intensifies hydroclimatic extremes across the UK and to inform regionally adaptive water management in a changing climate.

2 Study area and data

2.1 Study area and river flow data

This study focuses on the UK, which encompasses a wide range of hydrological, climatic, and landscape conditions. The UK's temperate maritime climate exhibits a pronounced northwest–southeast gradient in rainfall and temperature, shaped by prevailing westerlies, orographic uplift over western uplands, and rain-shadow effects in the east (Mayes and Wheeler 2013). Rainfall decreases and sunshine increases towards southeastern England, while mean temperatures shift from mild, wet conditions in the west and north to warmer, drier regimes in the southeast (Mayes and Wheeler 2013). These sharp contrasts across short distances make the UK a valuable testbed for assessing climate-driven changes in floods and droughts across temperate maritime environments.

A total of 698 catchments were analysed, including 668 from Great Britain (GB) based on the CAMELS-GB dataset (Catchment Attributes and MEteorology for Large-sample Studies; Coxon et al., 2020), and 30 catchments from Northern Ireland. The selected catchments represent a diverse range of sizes, topographies, and land uses, and span across all 23 UK River Basin Regions (RBRs), which serve as hydrologically defined units for climate impact assessments. Figure 1 shows the location of the catchments along with their river flow gauges and the RBRs they belong to. Daily streamflow observations for each catchment were obtained from the UK National River Flow Archive (NRFA).

Figure 1 The 668 CAMELS-GB catchments in Great Britain and 30 catchments in Northern Ireland, along with the river gauges overlaid on the UK's 23 River Basin Regions.

2.2 Climate forcing data

Historical meteorological data were obtained from the UK Met Office's HadUK-Grid dataset, which provides gridded daily precipitation and temperature observations at 1 km spatial resolution (Hollis et al. 2019). Potential evapotranspiration (PET) calculated using the Penman-Monteith equation was sourced from the CHESS-PE dataset (Robinson et al. 2023). These data were used for hydrological model calibration over the period 1990–2000.

Future climate projections were derived from the UK Climate Projections 2018 (UKCP18) Regional Climate Model (RCM) ensemble. This 12-member perturbed physics ensemble (PPE) was produced using the HadREM3-GA705 RCM at 12 km resolution (Murphy et al., 2018). The ensemble spans 100 years (1980–2080) and follows the high-emission scenario RCP8.5. For hydrological modelling, daily precipitation and temperature data were regridded to 1 km resolution and bias-corrected using an empirical quantile mapping method . The bias corrected climate projections were presented in Smith et al. (2024). PET projections were calculated using the Penman-Monteith equation and bias-corrected using the same method. The associated Python code is available via the repository listed in the Data and Code Availability section.

To align with global climate policy targets, we analysed hydrological responses at two warming levels, i.e. 2 °C and 4 °C above the pre-industrial (1850-1900) average. Specific 30-year periods corresponding to each warming level were selected for each ensemble member based on when global mean temperature anomalies reached the target warming thresholds, following Arnell et al. (2021). For ensemble members that exceeded the 2080 horizon before reaching 4 °C, the available years up to 2080 were used. Table 1 summarises the first year of a 30-year period in which each of the 12 UKCP18-RCM members reaches a certain warming level derived by Arnell et al. (2021).

Table 1 First year of 30-year period during which each UKCP18-RCM ensemble member reaches 2 °C and 4 °C global warming above pre-industrial levels, adapted from (Arnell et al. 2021).

Warming	01	04	05	06	07	08	09	10	11	12	13	15
2 °C	2016	2013	2018	2016	2017	2018	2014	2018	2015	2020	2016	2019
4 °C	2049	2046	2051	2049	2050	2055	2044	2052	2050	2052	2050	2054

This combination of high-resolution bias-corrected climate projections and nationally representative catchments provides a comprehensive framework for assessing future hydrological change across diverse UK regions.

3 Method

3.1 The HBV-TYN model

The HBV (Hydrologiska Byråns Vattenbalansavdelning) model (Bergström 1992; Lindström et al. 1997) was applied in this study. This conceptual rainfall-runoff model is widely used for flood forecasting and climate impact assessment (Arheimer et al. 2011; Cloke et al. 2013; He et al. 2022; Lidén and Harlin 2000; Olsson and Lindström 2008; van Pelt et al. 2009). Due to its robust performance across various catchments worldwide and its popularity among the hydrological research community, many different versions of the HBV model have been developed at different institutions.

The version used in this study is referred to as HBV-TYN, and based on the distributed HBV model (He et al. 2022) which was further developed from He et al. (2011). HBV-TYN consists of four key routines: (1) snowmelt and snow accumulation; (2) soil moisture and effective precipitation; (3) evapotranspiration; and (4) runoff response. The distributed HBV-TYN model can be set up at different spatial resolutions. In this study, the 1×1 km grid derived from the HadUK-Grid is used to align with the resolution of both observed and projected climate inputs (see Section 2.2). The 1 km resolution was deemed sufficient to represent the spatial variance of inputs and outputs while maintaining manageable computational and storage demands. It also facilitates comparison with other UK-wide hydrological models developed at 1 km resolution, such as G2G (Bell and Moore 1998; Bell et al. 2009), the DECIPHeR model (Coxon et al. 2019) and the SHETRAN model (Lewis et al. 2018; Smith et al. 2024).

Flow routing in HBV-TYN is implemented using the Muskingum method in a grid-to-grid framework, based on an 8-direction flow map derived from a 1×1 km Digital Elevation Model (DEM) of the UK. Due to the limitations in DEM resolution and elevation inaccuracies, manual corrections were required to ensure the flow directions correctly matched the surveyed river channels. These corrections ensured that all grid cells contributed flow within their respective catchments and routed to the designated outlet points. HBV-TYN runs at a daily time step and requires daily input data including precipitation (P), temperature (T), and potential evapotranspiration (ET).

In this study, the standard HBV model was adapted to incorporate representations of urban land cover and rainfall interception. Urban areas were represented as a percentage of each 1 km grid cell and used to estimate the fraction of precipitation that contributes directly to overland flow via impervious surfaces. The remaining effective precipitation was routed through the standard HBV pathways, including overland flow, interflow, and percolation. It is important to note this approach assumes urban areas are fully impervious, a simplification due to the lack of detailed spatial data on impervious surface fractions within each grid cell. Rainfall interception in both urban and forested areas was simulated following the approach described by Hundecha (2005). An interception storage capacity I_{max} was defined. Because the interception capacity of forests depends on their type and age as well as the seasons, I_{max} for urban and forest areas for each month were adopted from the values reported in Hundecha (2005).

3.2 Model Calibration and Evaluation

The model was calibrated over the period 1990-2000 using the meteorological inputs described in Section 2.2 and the daily observed discharge data obtained from the UK National River Flow Archive (NRFA). The first 365 days were used as the warm-up period. Table S4 in the Supporting Information lists the 9 calibrated parameters and their upper and lower bounds. The objective function used in the model calibration is the Nash–Sutcliffe Efficiency (NSE, (Nash and Sutcliffe 1970)) defined in the following equation.

$$\boldsymbol{NSE = 1 - \frac{\sum_{t=1}^{n}(Q_{o,t} - Q_{s,t})^2}{\sum_{t=1}^{n}(Q_{o,t} - \overline{Q_o})^2}}$$

where: n is the total number of observations, $Q_{o,t}$ and $Q_{s,t}$ are the observed and simulated flow at the t^{th} time-step, respectively, and $\overline{Q_o}$ is the mean of the observed flow. The NSE is a metric used to assess the predictive accuracy of hydrological models. An NSE value of 1 means perfect agreement between the model simulations and the observed data. An NSE value of 0 indicates the model's predictive capability is equivalent to using the mean of the observed data. If the NSE value is negative, it suggests the model performs worse than simply using the mean of the observations. In this study, a total of 50,000 Monte Carlo random parameter sets were generated and used for calibrating the model parameters. The parameter set achieving the highest NSE in the calibration period was retained as the optimal set. This method provides a straightforward and global search of the parameter space, avoiding sensitivity to initial guesses and the risk of local optima. Using the NSE allows consistent comparison with 7 other nation-wide models from three relevant studies, including Lane et al. (2019), Lees et al. (2021) and Smith et al. (2024).

3.3 Evaluation metrics

3.4.1 Precipitation extremes

To characterise hydroclimatic extremes relevant to both droughts and floods, we computed four metrics from the bias-corrected UKCP18 RCM ensemble outputs at 1 km grid resolution. These include maximum number of consecutive dry days (CDD_{max}), standardised precipitation index (SPI), maximum 1-day precipitation (RX1day), and the maximum 5-day precipitation (RX5day). Except for SPI, these metrics follow definitions recommended by the Expert Team on Climate Change Detection and Indices (Zhang et al. 2011). SPI is based solely on precipitation, making it a purer metric for meteorological droughts. An advantage of SPI is that it avoids conflating precipitation deficits with temperature-driven PET increases, which may or may not correspond to actual moisture stress. It is more widely used and recommended by WMO (World Meteorological Organization (WMO) and Global Water Partnership (GWP) 2016). It is often the standard baseline metric. For example, the UK Water Resources Portal reports monthly SPI, Standardised streamflow index (SSI) and Standardised groundwater index (SGI) as drought indices for monitoring not only dry but also wet periods. Collectively, the four metrics chosen in this study represent key aspects of hydroclimatic extremes including dry spell duration, meteorological drought severity, and short-duration precipitation extremes that may lead to flooding.

For each catchment and ensemble member, bias-corrected daily precipitation data were extracted at grid level for the 30-year baseline period (1981–2010) and the future 30-year periods corresponding to 2 °C and 4 °C global warming levels. $\mathrm{CDD}_{\max}$ was calculated as the longest sequence of days with precipitation below 1 mm for each 30-year period. SPI was computed at 3-, 6-, and 12-month accumulation scales using the gamma distribution fit to baseline monthly totals, and then applied to the two warming periods to enable standardised drought comparisons. SPI-3 and SPI-6 primarily reflect short-term meteorological and agricultural (soil-moisture) drought conditions, whereas SPI-12 captures longer-term hydrological stress, including sustained deficits that influence streamflow and groundwater recharge (Zhang et al. 2023; Sutanto et al. 2024). For SPI, the numbers of months where SPI < -1 (all drought) and SPI < -2 (extreme/severe) were used to assess the frequency and severity of dry periods. RX1day and RX5day represent the highest single-day and 5-day precipitation totals, respectively, and were computed from the daily data for the baseline and each warming level. The spatial averages of RX1day and RX5day across all grid cells within each catchment were calculated. All metrics were evaluated separately for the baseline, 2 °C, and 4 °C warming levels. Ensemble medians across 12 RCM members were used to summarise projected changes.

3.4.2 River flow percentiles

Percentage changes in daily river flows under 2 °C and 4 °C warming levels were assessed using flow exceedance percentiles, that are exceeded for 5% (Q05), 50% (Q50) and 95% (Q95) of the flow record, representing high, median, and low flows, respectively. The analysis was conducted for annual, summer (June–August), and winter (December–February) seasons in the following steps. For each of the 12 RCM ensemble members, daily simulated river flow time series were extracted. Q05, Q50, and Q95 values were computed annually for each of the five seasonal definitions over the 30-year baseline and future periods associated with 2 °C and 4 °C global warming levels. For each ensemble member, the median of the 30 annual values was calculated for each Q metric and season. The ensemble median was then derived across all 12 members for each metric, season, and warming level. Finally, percentage changes relative to the baseline were calculated for each Q metric under each warming scenario and for each season.

3.4.3 Return floods

A flood frequency analysis was performed by estimating return flood magnitudes using the Gumbel distribution fitted to annual maximum daily flow values. For each catchment and each of the 12 UKCP18-RCM ensemble members, annual maxima were extracted from daily discharge data over a 30-year baseline period (1981–2010), and from future 30-year periods associated with 2 °C and 4 °C global warming levels. The Probability-Weighted Moments (PWM) method (Greenwood et al. 1979) was used to fit the Gumbel distribution and estimate its location and scale parameters. These parameters were then used to calculate discharge values corresponding to 5-, 10-, 20-, 50-, and 100-year return periods. To quantify climate impacts, the return floods under 2 °C and 4 °C warming were compared to baseline values, and percentage changes were computed for each return period. Ensemble medians across all 12 members were used to summarise the projected changes for each catchment.

3.4.4 Standardised streamflow index (SSI)

To assess hydrological drought conditions across UK catchments, we computed the standardised streamflow index (SSI) using the three-parameter Tweedie distribution recommended by (Svensson et al. 2017). SSI is a relatively new indicator for characterising drought and is the only recommended drought index for streamflow drought monitoring in the Handbook of Drought Indicators and Indices (World Meteorological Organization (WMO) and Global Water Partnership (GWP) 2016).

The SSI was computed at a 1-month aggregation scale (SSI1) using monthly mean flows. For each catchment, daily discharge values were aggregated into monthly means. Using the 30-year baseline period (1981–2010), monthly flows were grouped by calendar month (e.g. all Januarys, all Februarys, etc.). For each month, the baseline flows were fitted to a Tweedie distribution using the maximum likelihood estimation method, implemented via the tweedie package in R. The fitted distribution parameters were then used to compute cumulative probabilities for both baseline and future monthly flows. These probabilities were transformed into standard normal deviates using the inverse of the standard normal cumulative distribution function, resulting in the SSI time series. SSI is used because it standardises streamflow anomalies relative to each catchment's baseline variability, allowing spatial aggregation and comparison across catchments with very different flow magnitudes and regimes.

The SSI values were computed for the baseline period and for two 30-year future periods representing 2 °C and 4 °C global warming levels. The resulting SSI time series were summarised to derive the mean SSI per catchment and 23 river basin regions. For each catchment and period, the mean SSI was then derived by averaging all monthly SSI values. Regional ensemble mean SSI values were derived by aggregating catchments within their respective River Basin Regions and compared across the baseline, 2 °C, and 4 °C warming levels to reveal projected changes.

Beyond its conventional use for drought monitoring, SSI1 can also serve as a useful indicator of short-term hydrological variability, making it suitable for detecting rapid transitions between dry and wet flow conditions, which is referred to as hydroclimatic whiplash. Hydroclimatic whiplash means abrupt and extreme shifts between opposing hydroclimatic states, such as droughts followed by floods or vice versa, within a short time frame. These events are increasingly recognised for their ecological, economic, and societal impacts, and have been studied mainly in terms of meteorological whiplash using precipitation-based indices such as the Standardised Precipitation Index (SPI) (e.g., Cheng and Liu 2022; Francis et al. 2022), Standardised Precipitation Evapotranspiration Index (Swain et al. 2025) and percentiles of standardised precipitation anomalies (Tan et al. 2023). However, precipitation-based indices alone do not capture the integrated hydrological response. Hydrological whiplash can be more accurately represented by streamflow-based indicators such as SSI, which integrates catchment processes and antecedent conditions. In this study, we focus on the 1-month SSI to detect abrupt transitions in river flow, capturing the direct hydrological impacts of rapid dry-to-wet or wet-to-dry swings. Two types of whiplash events are defined here. The immediate transition from SSI1 ≤ -1 (dry) to SSI1 ≥ 1 (wet) is defined as a dry-to-wet whiplash, and the opposite is a wet-to-dry whiplash. To our knowledge, this is the first study to apply the SSI for assessing hydrological whiplash changes under future climate warming scenarios.

4 Results and discussion

4.1 Model performance

The HBV-TYN model was calibrated for the period 1990-2000 using a Monte Carlo sampling of 50,000 parameter sets for each of the 698 UK catchments. The parameter set resulting in the highest NSE value was selected for each catchment. A total of 541 catchments achieved NSE $\geq$ 0.7, accounting for 77% of all the study catchments. The median NSE of all the 698 catchments is 0.81. Detailed spatial patterns, regional summaries, and benchmarking against 7 other nation-wide models are provided in Supporting Information Section A. It is worth noting here while NSE provides a robust overall measure of model performance and allows direct comparison with other national-scale studies, it can be more sensitive to high flows and less responsive to low-flow performance. A multi-objective calibration approach, such as combining NSE with Kling–Gupta Efficiency (KGE) or log-transformed NSE (NSE-log), could be used to better represent low-flow dynamics.

Of the 698 modelled catchments, 317 non-overlapping catchments are mapped to avoid duplication where smaller nested catchments are contained within larger ones. A list of non-overlapping catchments with NSE < 0.7 and their corresponding River Basin Regions is provided in Table S5. These catchments with lower calibration performance (e.g. in parts of the Thames and Anglian regions) have minimal influence on the projected relative changes because the same model structure and parameters are applied consistently across baseline and warming scenarios. The large-scale patterns and ensemble-median responses are dominated by well-performing catchments. Nevertheless, the results presented in Section 4.3 for the catchments with low model performance should be interpreted with caution, as local uncertainties are higher in groundwater-dominated or highly regulated catchments.

4.2 Projection of future precipitation

4.2.1 Maximum consecutive dry days ($\mathrm{CDD_{max}}$)

Figure 2 shows the maximum number of consecutive dry days ($\mathrm{CDD_{max}}$) across the UK catchments under (a) baseline, (b) 2 °C, and (c) 4 °C global warming levels. It was calculated as the median across 12 bias-corrected UKCP18 RCM ensemble members for each catchment. The colour scale represents the length of the longest dry spell (in days) during a 30-year period. Projected changes in $\mathrm{CDD_{max}}$ show a clear intensification of dry spells across the UK under global warming scenarios. Under baseline conditions, the national median of the maximum number of consecutive dry days is 32. This increases to 36 days under 2 °C warming and 41 days under 4 °C. Spatial patterns reveal the most pronounced increases in southern and southeastern England, where $\mathrm{CDD_{max}}$ commonly exceeds 50 days under 4 °C warming. These areas also exhibit the greatest absolute changes, with some catchments seeing increases of more than 20 days compared to the baseline. In contrast, catchments in northern and western Scotland show smaller increases, with $\mathrm{CDD_{max}}$ remaining below 35 days even under the highest warming scenario.

The pronounced northwest-southeast (NW–SE) gradient evident in $\mathrm{CDD}_{\max}$ reflects the combined influence of enhanced temperature-driven evaporative demand under warming, large-scale atmospheric circulation, and orographic rain-shadow effects. Southern and southeastern England warm more strongly and exhibit higher potential evapotranspiration, leading to more rapid depletion of soil moisture during dry periods. These regions are affected by persistent anticyclonic (blocking) conditions that restrict the passage of Atlantic frontal systems (Kendon et al. 2013; Lavers et al. 2015; Svensson et al. 2017) They are situated in the lee of the western uplands and receive reduced rainfall from westerly flows. The elevated evaporative losses further intensify surface drying (Kay 2021) and extend the duration of consecutive dry days. In contrast, northern and western regions, which are more frequently influenced by westerly airflow and orographic uplift associated with Atlantic frontal systems (Burt and Howden 2013), experience more frequent rainfall events that interrupt dry spells and therefore limit the duration of consecutive dry days. These combined processes explain why dry spells lengthen most strongly in southern and southeastern England while remaining shorter in upland and maritime regions in northwest.

These trends suggest that the risk of hydrological and agricultural droughts could intensify in already dry regions of southern and eastern England, including the Anglian, Thames, and South East River Basin Regions, indicating a heightened risk of prolonged drought conditions. The expansion of dry spells could place additional stress on water supply systems and ecosystems, especially during summer months.

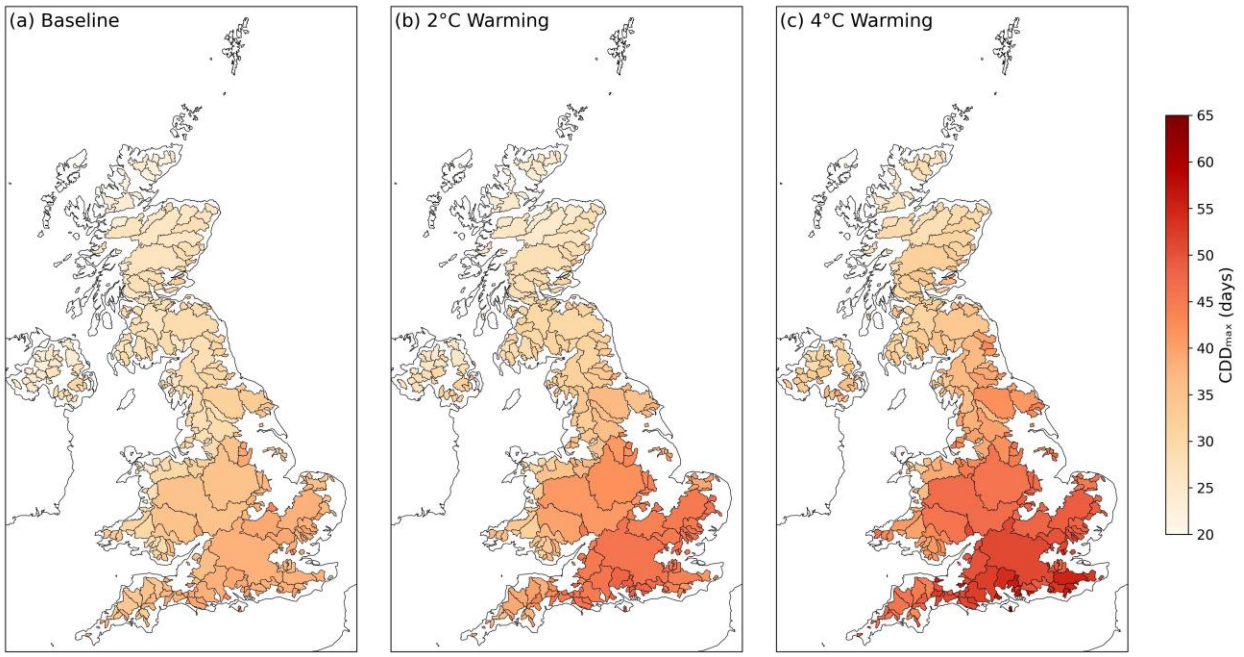

Figure 2 Maximum number of consecutive dry days ($\mathbf{CDD_{max}}$) across UK catchments under (a) Baseline, (b) 2 °C, and (c) 4 °C global warming levels. Maps show 317 non-overlapping representative catchments selected from the full 698 catchments to avoid overlap.

4.2.2 Standardised precipitation index (SPI)

Figure 3 shows the regional median frequencies of drought months (SPI < -1) across UK river basin regions under baseline, 2 °C, and 4 °C warming levels, based on SPI3, SPI6, and SPI12 computed using a fixed baseline climatology. Drought frequency values represent the percentage of individual months within the 30-year simulation period during which the SPI fell below the specified threshold (e.g. -1 or -2). A consistent and substantial increase in drought frequency (SPI < -1) is observed across all SPI timescales, particularly under 4 °C warming. The frequency of SPI3 drought months increases from a national median of 16.0% under the baseline to 17.9% at 2 °C and 23.5% at 4 °C. The most affected regions include South West England, South East England and Severn with SPI3 exceeding 29%. A frequency of 29% indicates that approximately 104 out of 360 months had SPI3 values below -1, meaning that nearly one in every three months concluded a three-month period of significantly below-average precipitation. These drought months may be clustered or scattered. SPI6 shows similarly increasing trends and similar magnitudes of drought frequencies. The three most affected regions are the same as those based on SPI3. SPI12, which reflects long-term hydrological droughts accumulated over a 12-month period, reveals regionally variable but consistently increasing drought frequency under warming scenarios. Under baseline conditions, the median frequency of SPI12 < -1 events across UK river basin regions is approximately 15.5%, increasing to 17.6% under 2 °C warming and further to 22.9% under 4 °C. The three regions with the highest SPI12 include Anglian, Dee and Northumbria, where drought frequency under 4 °C exceeds 28.9%. These changes indicate a substantial intensification of long-term water deficits in a warmer climate, potentially impacting reservoir storage, groundwater recharge, and cumulative soil moisture availability. While SPI3 and SPI6 reflect more immediate meteorological and agricultural drought signals, SPI12 captures compounded hydrological stress, which is especially relevant for water resource management and planning.

Some regions, such as Argyll, Clyde, and Solway, show contrasting behaviour across SPI timescales. Short-term drought frequencies (SPI-3 and SPI-6) increase under warming, reflecting more frequent short dry spells between intense rainfall events. This behaviour is consistent with enhanced precipitation intermittency, where heavier rainfall is delivered in fewer episodes overall but with higher intensities, leading to longer dry breaks between storms (Kendon et al. 2014). In contrast, SPI-12, which capturs long-term cumulative moisture deficits, shows smaller changes or even decreases in these western regions. This occurs because annual precipitation totals remain relatively stable or increase slightly, offsetting short-term deficits and preventing the development of prolonged hydrological drought. This divergence between short- and long-term SPI responses indicates a shift from sustained moisture deficits toward more variable, high-frequency hydroclimatic conditions. Such increased intermittency also aligns with the projected rise in dry-to-wet whiplash events discussed in Section 4.3.3.

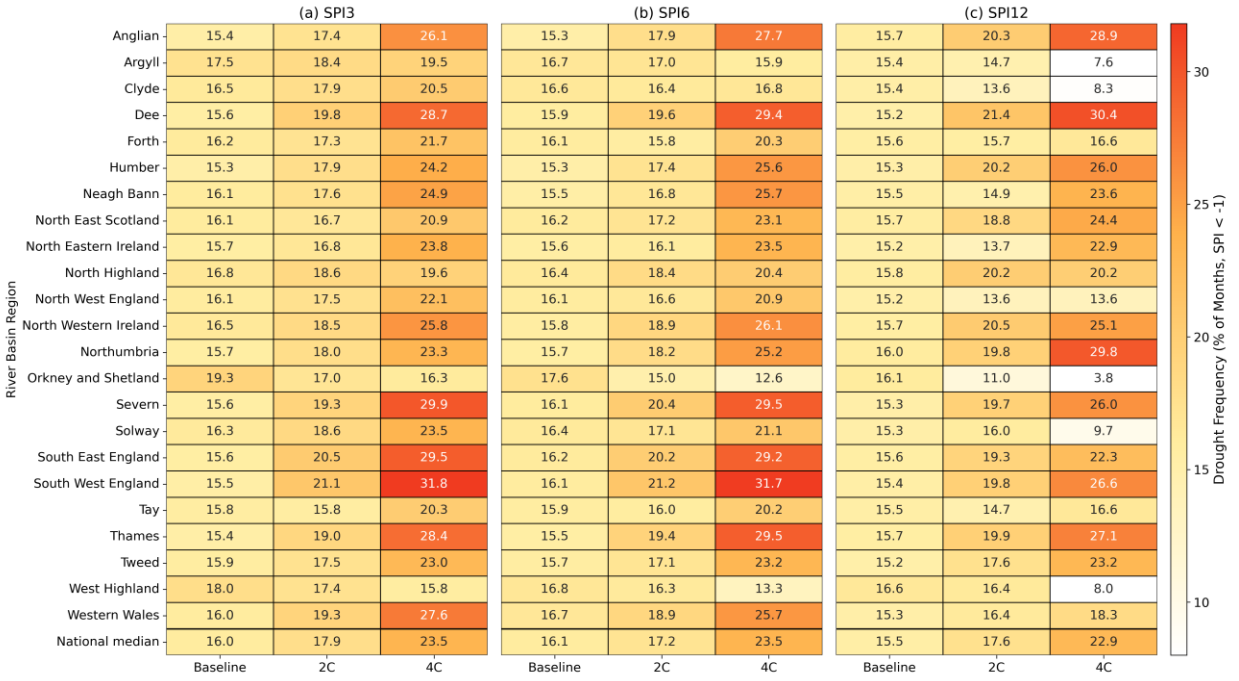

Figure 3 Regional median frequencies of drought months (SPI < -1) across UK river basin regions under baseline, 2 °C, and 4 °C warming levels, based on (a) SPI3, (b) SPI6, and (c) SPI12. National median values are included as the last row.

Frequency of extreme and severe droughts (SPI < -2) also increases markedly (see Figure S3 in the Supporting Information). The median SPI3 drought frequency rises from 2.3% (baseline) to 3.1% at 2 °C and 6.3% at 4 °C. Similar patterns are seen in SPI6, where regional drought frequencies of SPI 6< -2 reach up to 12.5% at 4 °C.

These findings are consistent with those of Reyniers et al. (2023), who also used the UKCP18 RCM ensemble and reported a significant increase in the frequency of SPI6 drought events across Great Britain. Their GB mean values of drought frequencies (SPI6 <-1) for baseline, 2 °C and 4 °C warming periods are 15%, 17% and 26% which are very close to the UK median values at 16.1%, 17.5% and 25% found in this study. Both studies reinforce the conclusion that drought risks intensify considerably with higher warming levels, particularly under 4 °C, highlighting the urgency of climate mitigation and adaptive water resources management.

4.2.3 Maximum 1-day and 5-day precipitation totals (RX1day and RX5day)

The maximum 1-day and 5-day precipitation totals (RX1day and RX5day) were evaluated for the baseline, 2 °C, and 4 °C warming levels. The UK-wide summaries of RX1day and RX5day indices (Table 2) show a consistent intensification of extreme precipitation events under 2 °C and 4 °C warming scenarios, relative to the baseline period (1981–2010). For RX1day, the UK-wide minimum (maximum) value increases from 25.95 (86.92) mm at baseline to 28.40 (105.86) mm at 2 °C and 29.20 (117.13) mm at 4 °C. The UK-wide mean RX1day increases by 4.58 mm at 2 °C and 7.89 mm at 4 °C, reaching 48.22 mm under the higher warming level. For RX5day, the UK-wide minimum rises modestly from 45.40 mm to 49.34 mm. The UK-wide maximum RX5day

reaches 225.54 mm under 4 °C warming, up from 199.54 mm in the baseline. The mean increases from 80.50 mm to 86.38 mm (+5.88 mm) at 2 °C and to 89.93 mm (+9.43 mm) at 4 °C. These results indicate a clear warming-related increase in the intensity of both short-duration (1-day) and multi-day (5-day) extreme precipitation events, with larger increases observed under higher warming levels.

Table 2 UK-wide minimum, maximum, and mean values in mm of RX1day and RX5day for the baseline, 2 °C, and 4 °C warming scenarios, including absolute changes from the baseline. NRFA Catchment IDs associated with the minimum and maximum changes are shown in parentheses.

Period	Minimum		Maximum		Mean	
	RX1day	RX5day	RX1day	RX5day	RX1day	RX5day
Baseline	25.95	45.40	86.92	199.54	40.33	80.50
2°C	28.40	48.87	105.86	208.96	44.91	86.38
2°C-Baseline	0.68 (30012)	-0.66 (96002)	18.94 (65001)	22.70 (73010)	4.58	5.88
4°C	29.20	49.34	117.13	225.54	48.22	89.93
4°C-Baseline	1.25 (25029)	-0.52 (96002)	30.21 (65001)	41.90 (65001)	7.89	9.44

Figure 4 shows the spatial distribution and projected changes in RX1day (top row) and RX5day (bottom row) across UK catchments under baseline, 2 °C, and 4 °C warming scenarios. Under baseline conditions, both indices are highest in the western and northern parts of the UK, particularly in western Scotland, the Lake District, and parts of Wales, where precipitation is strongly influenced by orographic uplift and Atlantic frontal systems. Under 2 °C and 4 °C warming scenarios, the projected changes are overwhelmingly positive, with notable intensification at 4 °C in northwest England, Wales, and western and southern Scotland. Eastern and southeastern catchments show more moderate changes although still exhibit widespread positive anomalies, indicating nation-wide intensification which could lead to increases in flooding risks. This NW–SE gradient is similar to the spatial pattern observed for CDD_{max}, but the underlying processes differ. For precipitation extremes, the contrast arises primarily from westerly airflow and orographic uplift in the western uplands, which intercept moist Atlantic air masses, producing larger increases in precipitation extremes, while eastern and southeastern lowlands in the lee receive smaller changes (Burt and Howden 2013; Mayes and Wheeler 2013). On the other hand, the $\mathrm{CDD}_{\max}$ pattern is driven by anticyclonic blocking, lee-side drying, and enhanced evaporative demand in southern and eastern England. Catchments with increases exceeding 20 mm are highlighted in blue outlines in the middle and right panels of Figure 4, indicating localised amplification of storm events in upland or flood-prone regions. The largest increases in RX1day and RX5day occur in catchment 065001 (Glaslyn at Beddgelert) in Snowdonia National Park, North Wales, with absolute increases of +30.21 mm and +41.90 mm, respectively, at 4 °C (see Table 4). A small number of catchments exhibit slight negative changes in RX5day, highlighted with red outlines in the middle and right panels of the bottom row. Specifically, two

483 catchments show decreases at 2 °C, and three at 4 °C, with reductions no greater than 0.66 mm,
484 suggesting these changes are negligible at the national scale. Because these small decreases
485 occur in only a few isolated catchments and show no spatial coherence, they are likely due to
486 sampling variability or numerical precision and should not be considered meaningful reductions
487 in extreme rainfall.

488 The projected increases in RX1day and RX5day align with recent findings from UK high
489 resolution climate simulations, which show that local extreme downpours intensify by 5–15% per
490 degree of warming and events exceeding 20 mm/h become four times as frequent by the 2070s
491 under high-emission scenarios (Kendon et al. 2023). These results reinforce that warming could
492 substantially increase the frequency and severity of short-duration extreme rainfall events across
493 the UK.

494

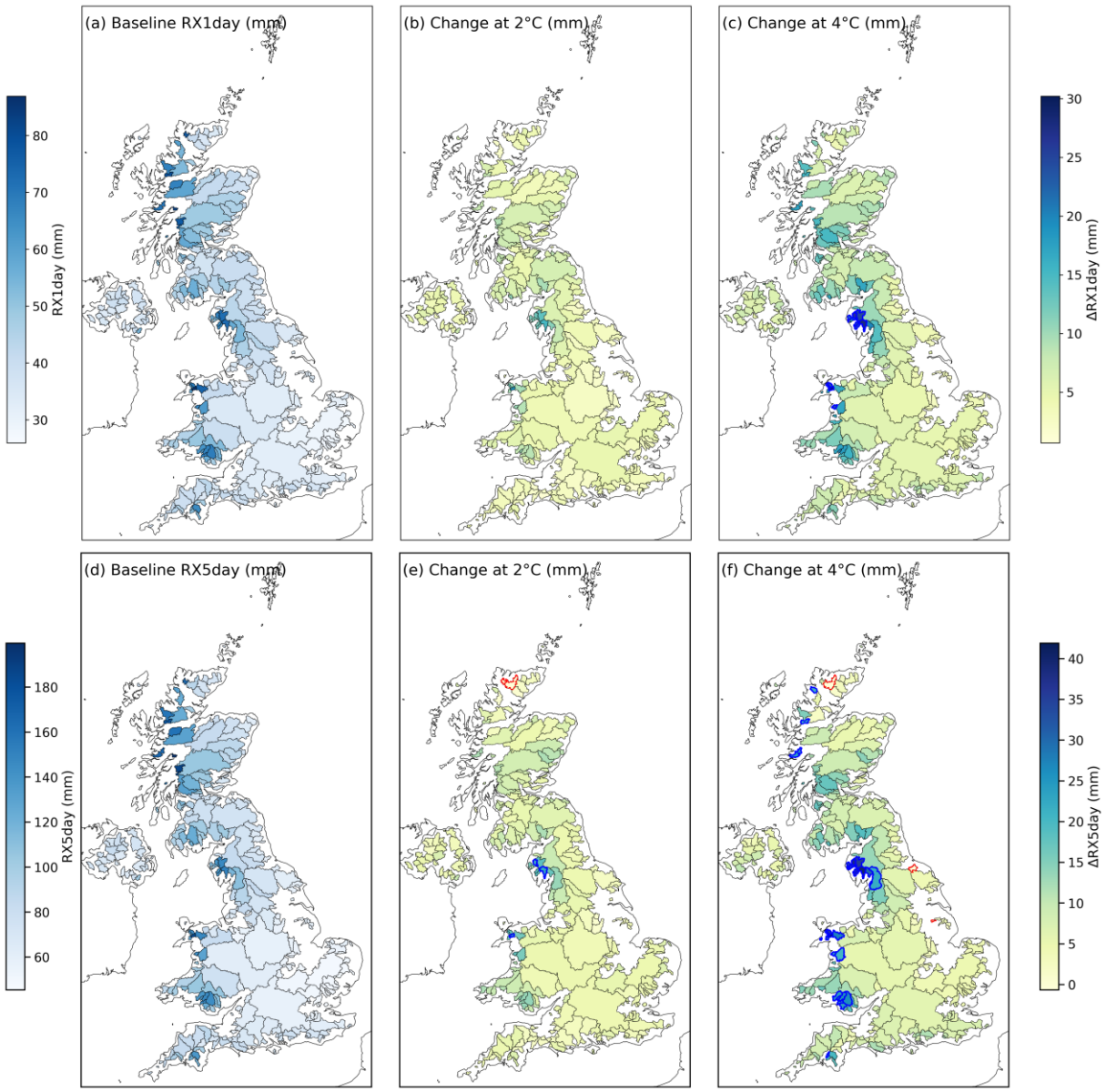

Figure 4 Spatial distribution of maximum 1-day precipitation (RX1day, top) and maximum 5-day precipitation (RX5day, bottom) across UK catchments under baseline and future warming scenarios: (a) Baseline RX1day; (b) Change in RX1day at 2 °C; (c) Change in RX1day at 4 °C; (d) Baseline RX5day; (e) Change in RX5day at 2 °C; and (f) Change in RX5day at 4 °C. Values are shown in millimetres. The catchments with changes > 20mm and negative changes are

503 highlighted with blue and red outlines, respectively. Maps show 317 non-overlapping
504 representative catchments selected from the full 698 catchments to avoid overlap.
505

506 ## 4.3 Projection of future flows

507 ### 4.3.1 River flow percentiles

508 Figure 5 shows projected percentage changes in Q05 (high flow), Q50 (median flow), and
509 Q95 (low flow) across UK catchments under a 4 °C warming scenario. Figure S4 in the Supporting
510 Information shows the same information under a 2 °C warming scenario. Changes are shown for
511 the annual average, as well as summer (June–August) and winter (December–February) seasons.
512 Red shades indicate reductions, and blue shades indicate increases in flow compared to the
513 baseline.

514 Q05 projections reveal an east–west contrast in high flow changes. Annual Q05 values
515 show moderate reductions across southern and eastern parts of the UK, while catchments in the
516 west, particularly in Wales and western Scotland, display increases, which likely reflects
517 enhanced orographic rainfall. This finding is consistent with Kay et al. (2021b), who reported that
518 5- and 20-year return period high flows are generally projected to increase across the UK, but
519 with notable decreases in southern and eastern regions, where uncertainties are also larger. But
520 they did not study seasonal differences. In summer, Q05 declines are widespread and
521 pronounced, indicating a marked reduction in high flow events during the dry season. Conversely,
522 winter Q05 exhibits large increases across western and northern regions, consistent with wetter
523 winter conditions and the intensification of high-flow extremes. The spatial correspondence
524 between precipitation extremes and high-flow responses is evident when comparing Figures 4
525 and 5. Regions showing the largest increases in annual RX5day, including the western uplands of
526 Wales, northwest England, and western Scotland, also exhibit substantial rises in annual high
527 flows (Q05) and flood return levels (see Figure 6). This reflects the dominance of steep, rainfall-
528 driven catchments where enhanced precipitation intensity directly amplifies flood peaks. In
529 contrast, southeastern and eastern catchments display modest increases in RX5day but clear
530 reductions in Q05 under 4 °C warming. These declines indicate that enhanced evaporative
531 demand and reduced antecedent soil moisture offset the effect of slightly heavier rainfall events,
532 leading to less runoff generation. These spatially contrasting patterns highlight a non-linear
533 hydro-climatic response: increases in rainfall extremes do not uniformly translate into higher
534 flood flows, but instead depend on regional water balance and catchment characteristics.

535 For Q50, a distinct north–south gradient is evident. Annual Q50 reductions are more
536 pronounced in southern and eastern catchments, which aligns with regional drying trends.
537 Summer Q50 declines are widespread and severe, frequently exceeding 40%, reflecting reduced
538 baseflows and lower overall water availability during the driest part of the year. In winter, Q50
539 responses are more spatially variable, with increases observed in central and western regions,
540 while eastern and southern England shows continued declines, suggesting that wetter winters
541 may not be uniformly distributed in the UK. These findings are consistent with earlier work by
542 (Arnell et al. 2021; Kay et al. 2020; Smith et al. 2024). They all project a pronounced decline in

543 summer flows and an increase in drought frequency in southern England. Smith et al. (2024) also
544 reported a nationwide reduction in median daily river flows.

545 Annual Q95 projections indicate substantial declines across much of the UK, reflecting a
546 widespread reduction in low flows. Summer Q95 shows a similar drying pattern, though the
547 magnitude of change is slightly less pronounced compared to annual values. These reductions in
548 low flows during the annual and summer periods align with the intensification of drought
549 conditions identified through increases in CDDmax and reductions in SPI discussed earlier. In
550 contrast, winter Q95 exhibits a more spatially variable pattern. A general trend toward wetter
551 conditions is observed in Wales, Northern Ireland, western England, and upland Scotland, where
552 winter low flows are projected to increase. However, southern and eastern England display
553 continued reductions in Q95 even during winter months. This is particularly concerning, as winter
554 is typically the period for aquifer and reservoir recharge. The persistence of low flows in these
555 regions could further exacerbate water resource stress, reducing resilience to subsequent dry
556 periods. These spatial patterns and regional contrasts are broadly consistent with those reported
557 by Kay (2021), who found that for 5- and 20-year return period low flows, most regions exhibited
558 decreasing trends, with only a few exceptions. Our study provides additional insights into
559 seasonal changes.

560

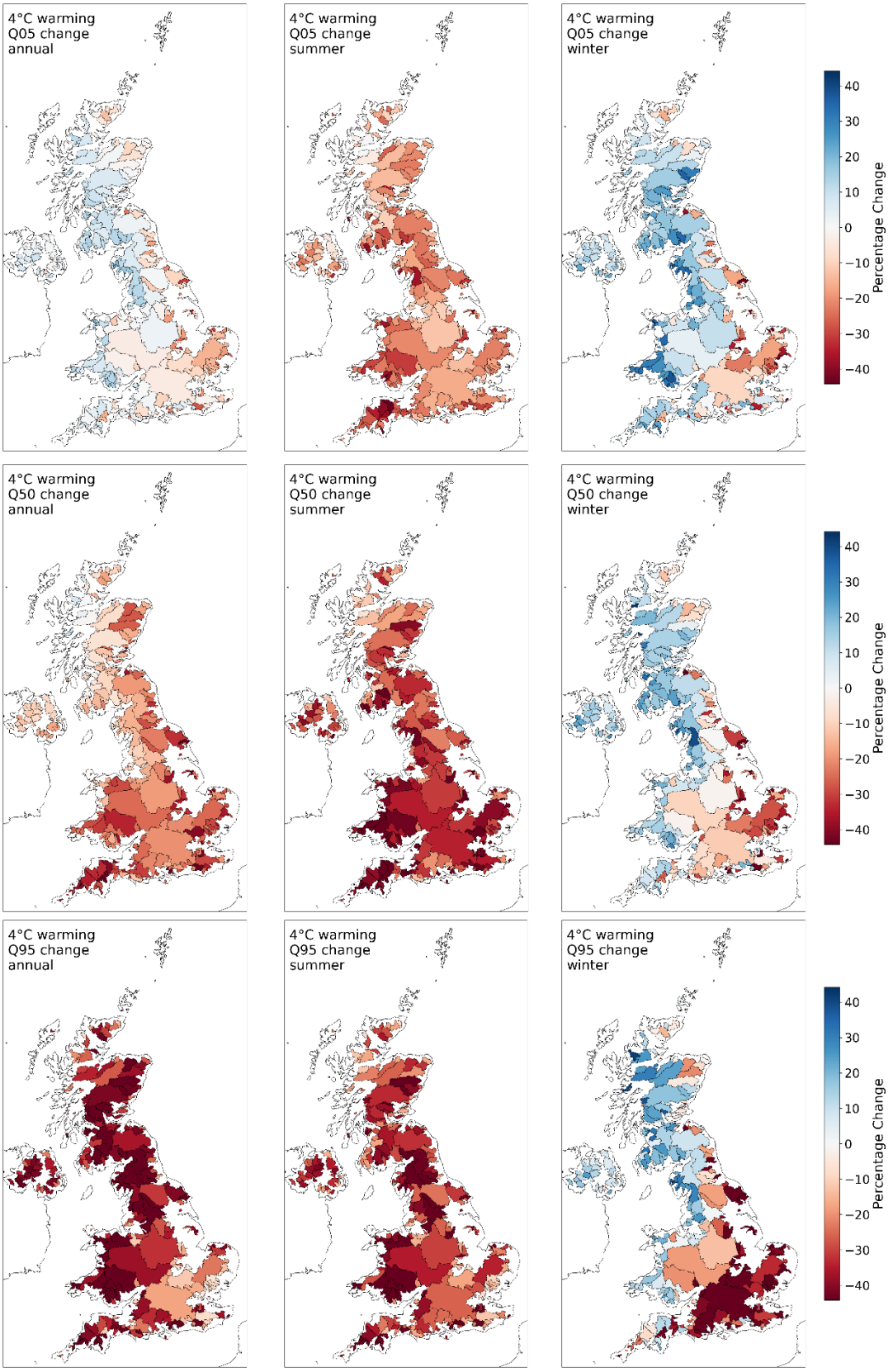
4°C warming
Q05 change
annual
4°C warming
Q05 change
summer
4°C warming
Q05 change
winter
4°C warming
Q50 change
annual
4°C warming
Q50 change
summer
4°C warming
Q50 change
winter
4°C warming
Q95 change
annual
4°C warming
Q95 change
summer
4°C warming
Q95 change
winter
40
30
20
10
0
−10
−20
−30
−40
Percentage Change

Figure 5 The percentage changes in river flows under a 4.0 °C warming level relative to the baseline period 1981-2010 for the 5th percentile flows (Q05, top row), median flows (Q50, middle row), 95th percentile flows (Q95, bottom row). The left, middle and right panels represent annual, summer, and winter seasons, respectively. Maps show 317 non-overlapping representative catchments selected from the full 698 catchments to avoid overlap.

4.3.2 Return floods

Projected changes in flood magnitudes for the 5-, 10-, 20-, 50-, and 100-year return periods were quantified. The 50-year return flood period is used here as an example that represent similar change patterns of the other return periods. Figure 6 shows the projected percentage changes in 50-year return floods for 23 UK river basin regions at 2 °C (left) and 4 °C (right). Each boxplot represents the distribution of percent changes across all ensemble member–catchment combinations within each region. The spread reflects the combined spatial and ensemble variability in future flood risk. The changes reveal a nonlinear and regionally variable response to warming across the UK. While many regions show increases under both 2 °C and 4 °C scenarios, the response is not amplified with higher warming. The magnitude of flood change is generally lower at 4 °C than at 2 °C. At 2 °C, most regional medians show increases in the range of 20–50%, whereas at 4 °C, the range lowers to 6–40%. At 4 °C, the interquartile spreads are also wider compared to 2 °C, and the interquartile ranges include zero or negative values in several regions. The five regions with the lowest increases at 4 °C are Anglian, Humber, Dee, Northumbria, and South West England, while the highest increases are found in North Eastern Ireland, Western Wales, North Western Ireland, Orkney and Shetland, and Neagh Bann.

The same trend is observed for the other return periods (see Figure S2 in the Supporting Information). Despite the expectation that flood hazards would intensify with warming, the median percentage change at 4 °C is often lower than at 2 °C, and in some regions the spread includes potential decreases in flood magnitudes. The uncertainty, represented by the interquartile ranges and whiskers, generally increases at 4 °C. This indicates greater variability in projected outcomes across both ensemble members and catchments, suggesting higher flood risk uncertainty under stronger warming. Interestingly, while Q05 decreases in many southeastern and eastern catchments under 4 °C warming, the 50-year return floods still increase (albeit less than at 2 °C). This apparent contrast arises because Q05 represents frequent high-flow conditions that are influenced by reductions in mean runoff and antecedent soil moisture, whereas return floods are driven by rare, high-intensity rainfall events. Under strong warming, enhanced evaporative demand can suppress moderate flows, but precipitation extremes continue to intensify, producing higher peak discharges during flood events. The smaller increase at 4 °C relative to 2 °C reflects the competing effects of rainfall intensification and catchment drying, leading to a non-linear response of flood magnitude to warming.

Our findings differ from those reported by Smith et al. (2024), who found that UK-wide median 10-year return flood flows remain relatively stable but decrease in some regions by approximately 15% at 2 °C and up to 50% at 4 °C, and uncertainty intervals broaden with warming. Although both studies show increasing uncertainties at higher warming levels, our results show positive median percentage changes in all regions, albeit with lower medians at 4 °C

603 than at 2 °C. One possible explanation for this divergence is the use of the SHETRAN model by
604 (Smith et al. 2024), which explicitly simulates groundwater and unsaturated zone processes. In
605 some regions, this may lead to greater infiltration and subsurface storage under warming,
606 thereby damping surface runoff and reducing simulated flood peaks,, especially under high
607 warming conditions. In contrast, the HBV-TYN hydrological model used in our study is more
608 responsive to surface runoff generation which can lead to a stronger translation of extreme
609 rainfall into peak flows. This contrast highlights the need for further investigation into how
610 different model structures represent hydrological processes under warming and how these
611 influence flood hazard projections. The contrast also underlines the importance of considering
612 multiple hydrological model structures when using projections to inform adaptation decisions,
613 as different models may emphasize different runoff-generation pathways under warming. The
614 HBV-TYN results presented here should therefore be interpreted as one plausible member of a
615 wider hydrological model ensemble rather than a definitive projection. Moreover, a projected
616 reduction in the fluvial flood magnitudes under stronger warming does not necessarily equate to
617 lower overall flood risk. This study does not capture surface water flooding, which is driven by
618 intense, short-duration rainfall events and may become more frequent with warming, especially
619 in urban areas where drainage systems can be easily overwhelmed. Dedicated metrics and
620 modelling would be required to assess changes in this distinct flood type and, more broadly, the
621 full spectrum of flooding.

622 While the UKCP18-RCM data provide an ensemble of daily-scale projections, future
623 research should incorporate convection-permitting models (CPMs) for higher-resolution
624 assessments of sub-daily river flows, particularly in urban settings where flash flood risk is
625 increasing.

626

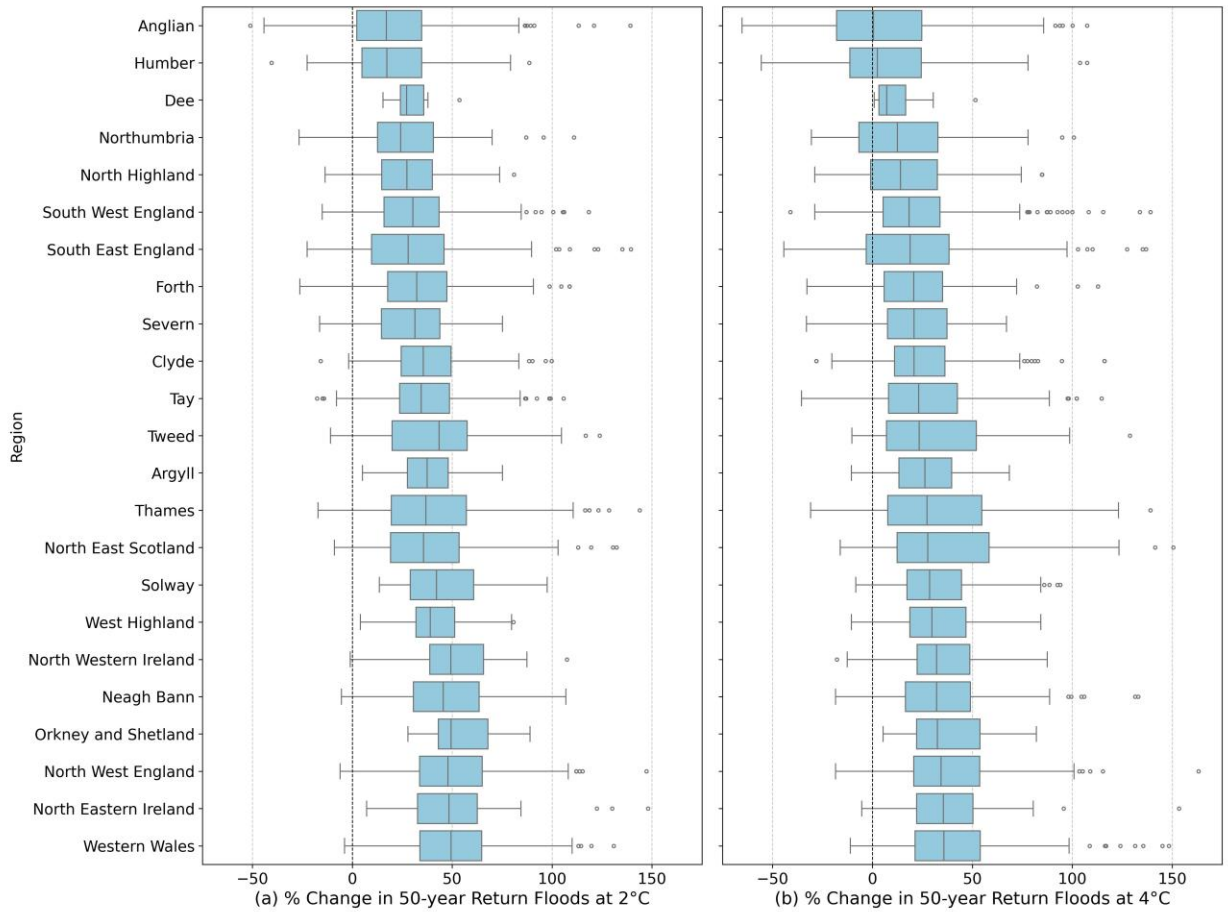

Figure 6 Projected percentage changes in 50-year return floods for 23 UK river basin regions under 2°C (a) and 4°C (b) warming scenarios. Each boxplot represents the distribution of percent changes across all ensemble member–catchment combinations within each region. The box represents the interquartile range (IQR, 25th–75th percentile), the line inside denotes the median, whiskers extend to 1.5×IQR, and circles represent outliers. Region ordering is based on the 4°C median to facilitate direct comparison.

4.3.3 Standardised streamflow index (SSI)

Figure 7 shows the regional changes in the 1-month Standardised Streamflow Index (SSI1) under baseline and future warming scenarios across UK River Basin Regions. Each subplot shows SSI trajectories for a specific River Basin Region under baseline, 2 °C, and 4 °C warming levels. Light grey lines represent individual catchments within the region, while the bold black line indicates the regional mean value across all catchments. Negative SSI values reflect increasingly dry streamflow conditions.

Across almost all regions, the regional mean SSI1 (bold black line) declines steadily from the baseline to 2 °C and then to 4 °C, indicating a widespread intensification of streamflow drought conditions as global temperatures rise. This trend is consistently observed across

individual catchments as shown by the downward-sloping grey lines, although the magnitude and spread of change vary by region.

The most pronounced declines are found in southern and eastern regions, particularly South East England, Thames, Humber, South West England, and Anglian where regional mean SSI1 approaches or falls below –0.5 at 4 °C warming. In some catchments, values approach –1.0, suggesting potential for moderate to severe hydrological drought. These regions are already subject to both high water demand and seasonal deficits, and future warming could exacerbate existing pressures on water supply, river ecology, and drought resilience.

The declining pattern is not uniform across the UK. While most catchments experience drying, several northern and western upland catchments show different trends. Orkney and Shetland exhibit a distinct increase in SSI1 with warming, suggesting a shift toward wetter streamflow conditions. Similarly, several catchments in the West Highland and North Highland regions also show positive changes in SSI1, despite the regional mean still showing a slight downward trend. These increases may be driven by enhanced winter precipitation, relatively low evapotranspiration losses, and the influence of a maritime climate that buffers against summer drying.

The spread among catchments (grey lines) increases with warming, particularly in eastern and southern England, indicating growing intra-regional variability in drought response. This underscores the importance of catchment-specific assessments, as regional averages can mask important local differences. Our results corroborate the recent drought assessment by Reyniers et al. (2023), who found that drought risk increases almost everywhere across Great Britain with rising global mean surface temperatures, and southern and eastern England are particularly vulnerable to concurrent and prolonged droughts under high-emissions scenarios. Reyniers et al. (2023) further demonstrate that multi-year drought events may become more frequent and severe based on the Standardised Precipitation Evapotranspiration Index (SPEI).

The projected SSI anomalies highlight the need to integrate climate-driven hydrological drought risks into long-term water resource management and drought resilience planning. In particular, regions that are already experiencing seasonal water stress are likely to see a compounding of risk under 4°C warming, necessitating adaptation strategies that are able to account for both short-term drought shocks and long-term chronic low-flow conditions.

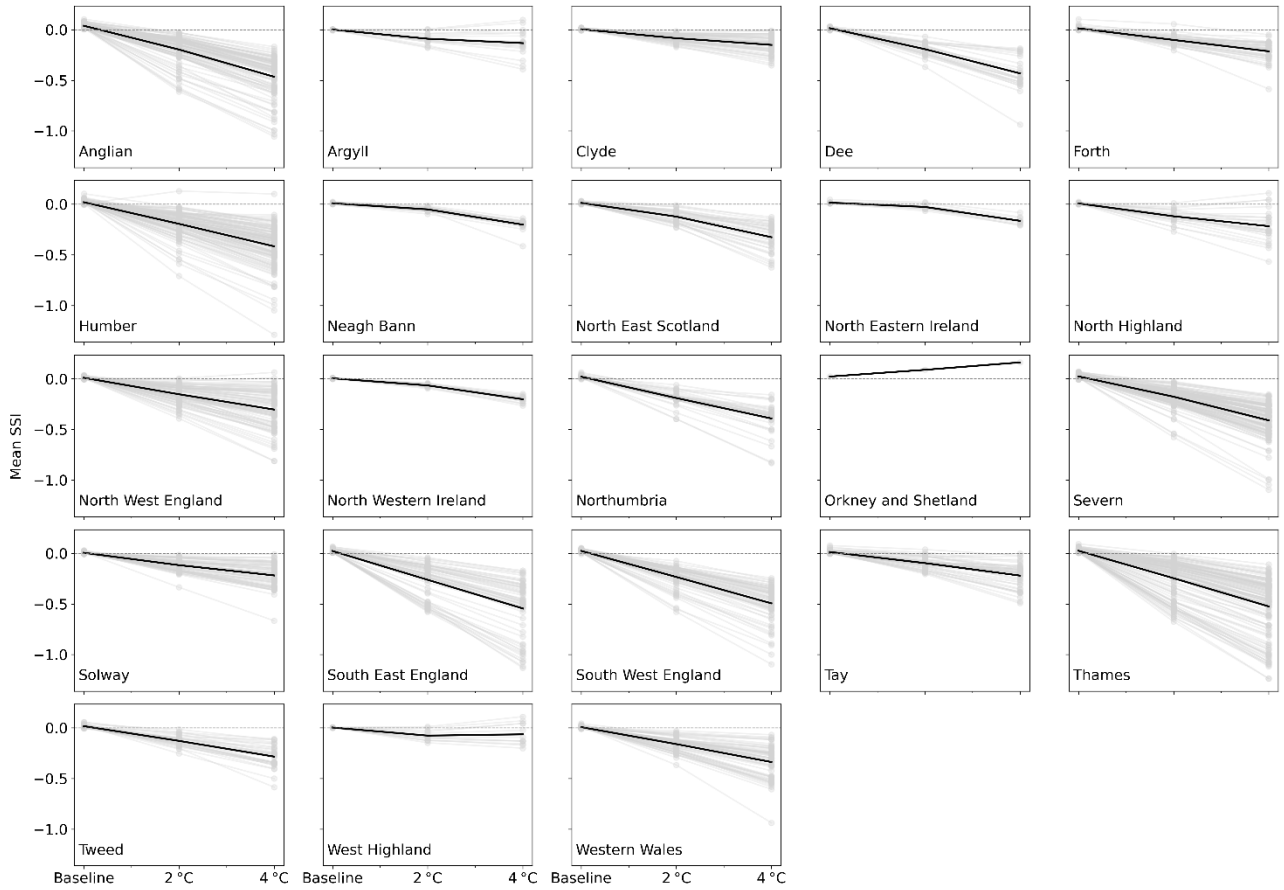

Figure 7 1-month Standardised Streamflow Index (SSI1) under baseline and future warming scenarios across UK River Basin Regions. Light grey lines represent individual catchments within the region, while the bold black line indicates the regional mean value across all catchments. Negative SSI values reflect increasingly dry streamflow conditions.

We also used the SSI1 index to assess baseline and future whiplash events for dry-to-wet and wet-to-dry transitions. Figure 8 shows the ensemble mean number of hydrological whiplash events across UK catchments under baseline, 2 °C and 4 °C warming levels. Results reveal that dry-to-wet whiplash events are, on average, more frequent than wet-to-dry events across UK catchments, with high baseline occurrences in western and northern regions such as western Scotland, Wales, and Northern Ireland. These areas, despite being generally wet, are hydrologically dynamic and prone to rapid transitions due to orographic rainfall and the influence of Atlantic frontal systems.

Projected changes under both 2°C and 4°C warming scenarios show widespread increases in the frequency of both types of whiplash events. For dry-to-wet whiplash, widespread increases can be seen across most of the UK, with some catchments showing +3 to +5 events at 4°C warming. Stronger increases can be observed in South Wales, Northern Ireland, Northern and Western England and parts of southeast England. The increases likely reflect intensified

hydrological variability as a result of warming. The simultaneous increase in the frequency of more negative SSI anomalies and more positive SSI anomalies suggests a widening spread of hydrological states. The projected increases in both types of anomalies therefore indicate a greater likelihood of threshold-crossing transitions between unusually dry and unusually wet conditions, reflecting intensifying hydrological whiplash under warming. The wet-to-dry whiplash also increases with warming but to a lesser extent than dry-to-wet and more spatially variable. The increase could be due to a warmer climate enhancing evapotranspiration and accelerating soil drying after wet periods, thereby increasing the frequency of wet-to-dry transitions.

Dry-to-wet whiplash may lead to flash flooding, water quality deterioration, and soil erosion, while wet-to-dry whiplash can challenge drought preparedness following misleading wet conditions. These findings highlight an emerging intensification of hydroclimatic variability under warming, with implications for flash flood risk, water quality, and drought resilience. It is worth noting a formal drought was declared on 29 May 2025 for North West England (UK Government 2025), only three years after a previous drought declaration in 2022. This underscores the region's increasing exposure to water scarcity despite its traditionally wet climate. Such conditions can arise when persistent high-pressure systems over the North Atlantic block westerly moisture-laden airflows, reducing rainfall over western UK regions. Compared to catchments in southern and eastern UK, norther and western catchments are flashier catchments with fast surface runoff response and limited groundwater storage, which can result in flash droughts when evaporative demand is high in warm months (Otkin et al. 2018; Barker et al. 2019, 2024). In our analysis, western and northern regions stand out as hotspots for increasing dry-to-wet whiplash events, suggesting that rapid transitions from drought to intense rainfall may become more common in a warming climate. These abrupt swings can pose significant challenges for water resources management, particularly for reservoir operations, by shortening the window for effective drought mitigation and increasing the risk of rapid inflows and overflow events during recovery. Water resource planning should therefore consider not just long-term mean flows but also the growing risk of sudden hydrological transitions and their implications for storage, treatment, and supply reliability.

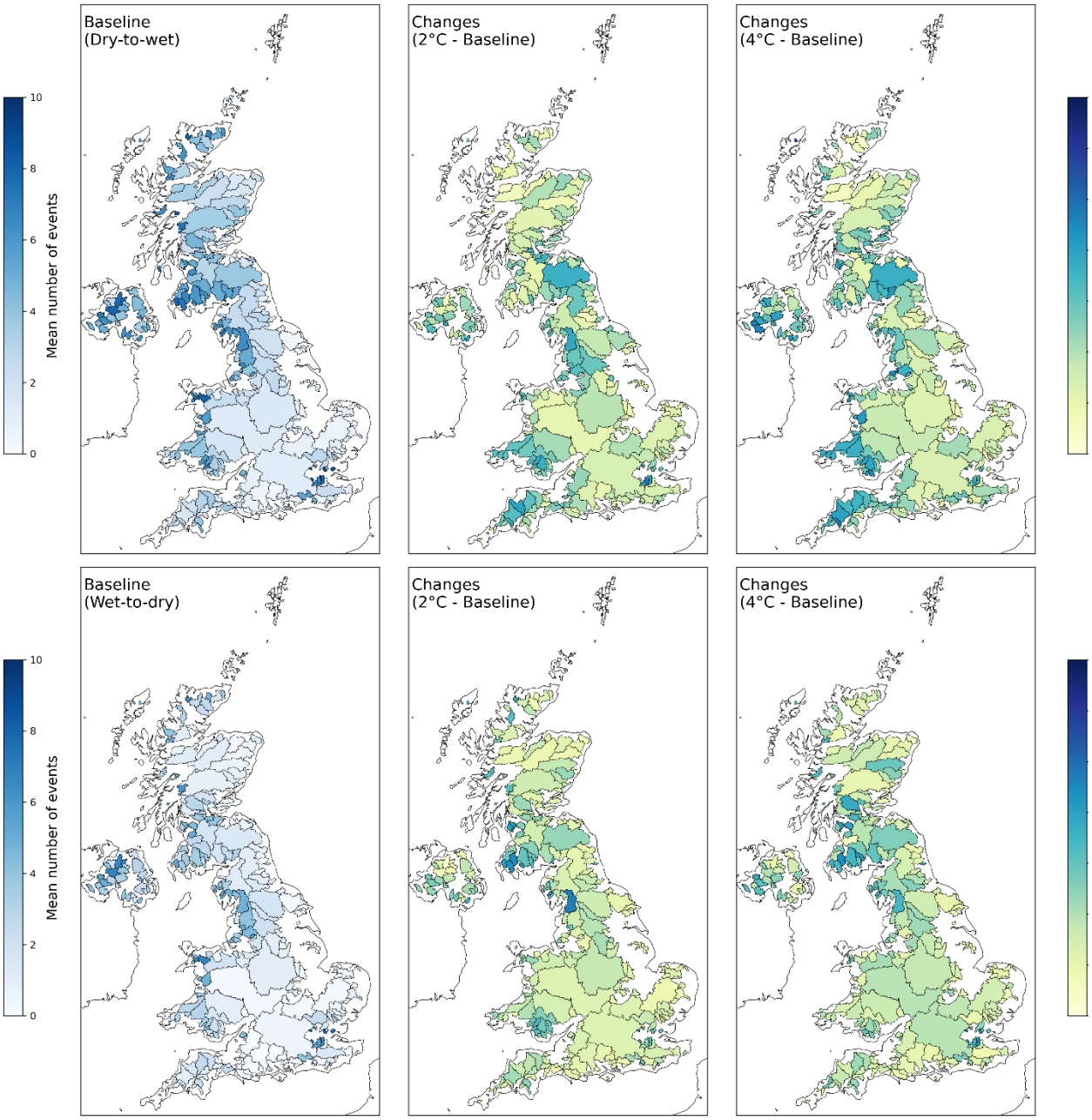

Figure 8 Spatial distribution of number of whiplash events across UK catchment. Top row: whiplash events from drought to wet. Bottom row: whiplash events from drought to wet. Left panel: Mean number of events during the baseline period (1981-2010). Middle panel: Absolute change (2 °C – baseline) under a 2 °C warming scenario. Right panel: Absolute change (4 °C – baseline) under a 4 °C warming scenario. Maps show 317 non-overlapping representative catchments selected from the full 698 catchments to avoid overlap.

An important source of uncertainty in our projections arises from the use of the UKCP18 Regional (12 km) climate ensemble, which samples internal variability and parameter uncertainty within a single GCM (HadGEM3-GC3.05) but does not capture the wider structural spread found

in multi-model ensembles. Numerous studies have shown that GCM structural differences are often the largest contributor to uncertainty in hydrological climate-change impact assessments (e.g. Chegwidden et al., 2019; Fatichi et al., 2016). The UKCP18 Science Report (Murphy et al. 2018) shows that, while the Regional PPE exhibits a consistent summer-drying signal over the UK, the CMIP5 multi-model ensemble includes members projecting substantially weaker summer drying or even increases in summer precipitation, and some models also simulate much larger winter precipitation increases than those represented in the Regional product (Murphy et al., 2018; Sections 4.5 and 5.1). The Report indicates the broader response ranges in Strands 1 and 2 arise from the influence of CMIP5 models, particularly over England where CMIP5 includes a few projections with increasing summer precipitation, whereas the PPEs show only decreases. The report also notes that Strand 3 samples the broader outcome space more narrowly, particularly in summer. These differences indicate that our projections may not fully represent the range of plausible hydroclimatic futures, particularly the possibility of less pronounced summer drying in southern and eastern regions and stronger winter wetting in western uplands. It highlights the need for future work using multi-GCM ensembles to better characterise the broader range of plausible hydroclimatic futures.

Because the UKCP18 RCM ensemble is a small, non-independent perturbed-parameter ensemble derived from a single GCM, formal statistical significance testing is not appropriate (von Storch and Zwiers 2013; Clark et al. 2016). We therefore interpret large-scale, spatially coherent ensemble signals rather than applying hypothesis tests, noting that a formal robustness or significance assessment would require a larger multi-GCM ensemble.

5 Conclusions

This study provides a comprehensive assessment of projected changes in UK river flows under 2 °C and 4 °C global warming scenarios, using bias-corrected UKCP18-RCM data and a distributed HBV-TYN hydrological model applied to 698 UK catchments. We employed a suite of hydrometeorological and hydrological metrics to evaluate both drought and flood hazards. Hydrometeorological metrics, including the longest consecutive dry days (CDD_{max}), the standardised precipitation index (SPI), and maximum 1-day and 5-day precipitation totals (RX1day and RX5day), were derived from bias-corrected ensemble projections at 1 × 1 km resolution and summarised at the catchment scale. Projected changes in river flows were evaluated using exceedance percentiles (Q05, Q50, Q95), return flood magnitudes (5-, 10-, 20-, 50-, and 100-year events), and the standardised streamflow index (SSI).

Our results reveal a regionally divergent intensification of extremes, with intensified short-duration rainfall events (for floods) and lengthened dry spells and precipitation deficits (for droughts) leading to greater hydroclimatic variability across UK catchments. Projected increases in daily and multi-day precipitation extremes (RX1day, RX5day) coincide with amplified high flows and flood magnitudes in western and northern uplands. This spatial pattern reflects the combined influence of large-scale westerly circulation and orographic uplift that sustain frequent rainfall in the northwest, in contrast to the lee-side drying and stronger evaporative demand in southern and eastern England under persistent high-pressure systems. Consequently, southern and eastern England exhibit longer and more frequent dry spells ($\mathrm{CDD}_{\max}$) and persistent streamflow deficits (Q95, SSI), reflecting growing drought exposure. The spatial contrast between

775 flood-dominated northwest regions and drought-prone southeast regions strengthens under
776 warming, reinforcing a pronounced northwest–southeast divide in UK hydroclimate.

777 More shifts between intense rainfall and prolonged dry periods indicate rising
778 hydroclimatic volatility, including an increasing frequency of whiplash events marked by rapid
779 alternations between wet and dry extremes. These transitions compound management
780 challenges by simultaneously stressing flood-defence and drought-response systems. The
781 findings underscore the need for regionally tailored adaptation, including enhanced flood-risk
782 management and nature-based storage solutions in western and northern regions, and
783 strengthened water-supply resilience and demand management in southern and eastern regions.
784 These measures should be supported by the development of dual-purpose infrastructure capable
785 of addressing the increasing occurrence of hydroclimatic whiplash events, alongside updated
786 hydrological design standards and integrated risk planning to manage the full spectrum of
787 hydrological extremes.

788 While some catchments, particularly in groundwater-dominated or heavily regulated
789 basins, show lower calibration performance, most catchments achieve good model performance,
790 which increases confidence in the large-scale spatial patterns identified. The consistent
791 application of the same model structure and parameters across scenarios supports the
792 robustness of the main conclusions. Future work could improve the model's representation of
793 groundwater–surface-water interactions and human regulation. It could also expand the forcing
794 data to include multi-model climate ensembles to better sample structural uncertainty, and
795 incorporate higher-resolution convection-permitting model projections to more accurately
796 represent extremes at both daily and sub-daily resolutions. Although NSE was used for calibration
797 to ensure methodological consistency across catchments and comparability with other UK-wide
798 models, it gives greater weight to high-flow conditions. Using a multi-objective calibration
799 approach that integrates low-flow-sensitive metrics (e.g., KGE or NSE-log) could improve the
800 simulation of drought-related processes. Future work could also explore the integration of
801 explainable or physics-informed machine learning models, which combine data-driven learning
802 with hydrological process constraints to improve interpretability and robustness under changing
803 climate conditions.

804

805 **Open Research**

806 The simulated discharge timeseries for all study catchments are available in (Newcastle
807 University and University of East Anglia 2024). The summary metric dataset used in this study is
808 available in (Newcastle University 2024). The River Basin Regions shapefile is accessible via the
809 UKCP18 spatial datasets (UKCP18). Daily streamflow observations for each catchment are
810 available from the UK National River Flow Archive (NRFA). The PET projection calculation and
811 bias-correction codes used in this work are openly available in (UKCP18-PET-BC).

812

Funding

This work was supported by the Open CLimate IMpacts modelling framework (OpenCLIM) project funded by the UK Natural Environment Research Council award number NE/T013931/1.

Conflict of Interest Statement

The authors declare that they have no financial or non-financial conflicts of interest that could have influenced the results, interpretations, or conclusions presented in this manuscript. All sources of funding that supported this research have been fully acknowledged. All authors have reviewed and approved this conflict-of-interest disclosure.

References

Arheimer B, Lindström G, Olsson J (2011) A systematic review of sensitivities in the Swedish flood-forecasting system. Atmospheric Research 100:275–284. https://doi.org/10.1016/j.atmosres.2010.09.013

Arnell NW, Kay AL, Freeman A, et al (2021) Changing climate risk in the UK: A multi-sectoral analysis using policy-relevant indicators. Climate Risk Management 31:100265. https://doi.org/10.1016/j.crm.2020.100265

Barker LJ, Hannaford J, Magee E, et al (2024) An appraisal of the severity of the 2022 drought and its impacts. Weather 79:208–219. https://doi.org/10.1002/wea.4531

Barker LJ, Hannaford J, Parry S, et al (2019) Historic hydrological droughts 1891–2015: systematic characterisation for a diverse set of catchments across the UK. Hydrology and Earth System Sciences 23:4583–4602. https://doi.org/10.5194/hess-23-4583-2019

Bell VA, Kay AL, Jones RG, et al (2009) Use of soil data in a grid-based hydrological model to estimate spatial variation in changing flood risk across the UK. Journal of Hydrology 377:335–350. https://doi.org/10.1016/j.jhydrol.2009.08.031

Bell VA, Moore RJ (1998) A grid-based distributed flood forecasting model for use with weather radar data: Part 1. Formulation. Hydrology and Earth System Sciences 2:265–281. https://doi.org/10.5194/hess-2-265-1998

Bergström S (1992) The HBV model: its structure and applications. SMHI Hydrology, Norrkoping, Sweden

Burt TP, Howden NJK (2013) North Atlantic Oscillation amplifies orographic precipitation and river flow in upland Britain. Water Resources Research 49:3504–3515. https://doi.org/10.1002/wrcr.20297

Chegwidden OS, Nijssen B, Rupp DE, et al (2019) How Do Modeling Decisions Affect the Spread Among Hydrologic Climate Change Projections? Exploring a Large Ensemble of Simulations Across a Diversity of Hydroclimates. Earth's Future 7:623–637. https://doi.org/10.1029/2018EF001047

Cheng L, Liu Z (2022) Detectable Increase in Global Land Areas Susceptible to Precipitation Reversals Under the RCP8.5 Scenario. Earth's Future 10:e2022EF002948. https://doi.org/10.1029/2022EF002948

Clark MP, Wilby RL, Gutmann ED, et al (2016) Characterizing Uncertainty of the Hydrologic Impacts of Climate Change. Curr Clim Change Rep 2:55–64. https://doi.org/10.1007/s40641-016-0034-x

Cloke HL, Wetterhall F, He Y, et al (2013) Modelling climate impact on floods with ensemble climate projections. QJR Meteorol Soc 139:282–297. https://doi.org/10.1002/qj.1998

Coxon G, Freer J, Lane R, et al (2019) DECIPHeR v1: Dynamic fluxEs and ConnectIvity for Predictions of HydRology. Geoscientific Model Development 12:2285–2306. https://doi.org/10.5194/gmd-12-2285-2019

Fatichi S, Ivanov VY, Paschalis A, et al (2016) Uncertainty partition challenges the predictability of vital details of climate change. Earth's Future 4:240–251. https://doi.org/10.1002/2015EF000336

Francis JA, Skific N, Vavrus SJ, Cohen J (2022) Measuring "Weather Whiplash" Events in North America: A New Large-Scale Regime Approach. Journal of Geophysical Research: Atmospheres 127:e2022JD036717. https://doi.org/10.1029/2022JD036717

Greenwood JA, Landwehr JM, Matalas NC, Wallis JR (1979) Probability weighted moments: Definition and relation to parameters of several distributions expressable in inverse form. Water Resources Research 15:1049–1054. https://doi.org/10.1029/WR015i005p01049

He Y, Bárdossy A, Zehe E (2011) A catchment classification scheme using local variance reduction method. Journal of Hydrology 411:140–154. https://doi.org/10.1016/j.jhydrol.2011.09.042

He Y, Manful D, Warren R, et al (2022) Quantification of impacts between 1.5 and 4 °C of global warming on flooding risks in six countries. Climatic Change 170:15. https://doi.org/10.1007/s10584-021-03289-5

Hollis D, McCarthy M, Kendon M, et al (2019) HadUK-Grid—A new UK dataset of gridded climate observations. Geoscience Data Journal 6:151–159. https://doi.org/10.1002/gdj3.78

Hundecha Hirpa Y (2005) Regionalization of parameters of a conceptual rainfall runoff model

Kay AL (2021) Simulation of river flow in Britain under climate change: Baseline performance and future seasonal changes. Hydrological Processes 35:e14137. https://doi.org/10.1002/hyp.14137

Kay AL, Davies HN, Lane RA, et al (2021) Grid-based simulation of river flows in Northern Ireland: Model performance and future flow changes. Journal of Hydrology: Regional Studies 38:100967. https://doi.org/10.1016/j.ejrh.2021.100967

Kay AL, Watts G, Wells SC, Allen S (2020) The impact of climate change on U. K. river flows: A preliminary comparison of two generations of probabilistic climate projections. Hydrological Processes 34:1081–1088. https://doi.org/10.1002/hyp.13644

Kendon EJ, Fischer EM, Short CJ (2023) Variability conceals emerging trend in 100yr projections of UK local hourly rainfall extremes. Nat Commun 14:1133. https://doi.org/10.1038/s41467-023-36499-9

Kendon EJ, Roberts NM, Fowler HJ, et al (2014) Heavier summer downpours with climate change revealed by weather forecast resolution model. Nature Clim Change 4:570–576. https://doi.org/10.1038/nclimate2258

Kendon M, Marsh T, Parry S (2013) The 2010–2012 drought in England and Wales. Weather 68:88–95. https://doi.org/10.1002/wea.2101

Lane RA, Coxon G, Freer JE, et al (2019) Benchmarking the predictive capability of hydrological models for river flow and flood peak predictions across over 1000 catchments in Great Britain. Hydrology and Earth System Sciences 23:4011–4032. https://doi.org/10.5194/hess-23-4011-2019

Lavers DA, Hannah DM, Bradley C (2015) Connecting large-scale atmospheric circulation, river flow and groundwater levels in a chalk catchment in southern England. Journal of Hydrology 523:179–189. https://doi.org/10.1016/j.jhydrol.2015.01.060

Lees T, Buechel M, Anderson B, et al (2021) Benchmarking data-driven rainfall–runoff models in Great Britain: a comparison of long short-term memory (LSTM)-based models with four lumped conceptual models. Hydrology and Earth System Sciences 25:5517–5534. https://doi.org/10.5194/hess-25-5517-2021

Lewis E, Birkinshaw S, Kilsby C, Fowler HJ (2018) Development of a system for automated setup of a physically-based, spatially-distributed hydrological model for catchments in Great Britain. Environmental Modelling & Software 108:102–110. https://doi.org/10.1016/j.envsoft.2018.07.006

Lidén R, Harlin J (2000) Analysis of conceptual rainfall–runoff modelling performance in different climates. Journal of Hydrology 238:231–247. https://doi.org/10.1016/S0022-1694(00)00330-9

915 Lindström G, Johansson B, Persson M, et al (1997) Development and test of the distributed
916 HBV-96 hydrological model. Journal of Hydrology 201:272–288.
917 https://doi.org/10.1016/S0022-1694(97)00041-3

918 Mayes J, Wheeler D (2013) Regional weather and climates of the British Isles - Part 1:
919 Introduction. Weather 68:3–8. https://doi.org/10.1002/wea.2041

920 Murphy JM, Harris GR, Sexton DMH, et al (2018) UKCP18 Land Projections: Science Report

921 Nash JE, Sutcliffe JV (1970) River flow forecasting through conceptual models part I — A
922 discussion of principles. Journal of Hydrology 10:282–290.
923 https://doi.org/10.1016/0022-1694(70)90255-6

924 Newcastle University (2024): OpenCLIM - Catchment Flow Metrics. NERC EDS Centre for
925 Environmental Data Analysis, *26 July 2024*. [Dataset]
926 doi:10.5285/81567bfb789e4ec4ae30cdd3772f8242. https://dx.doi.org/10.5285/81567b
927 fb789e4ec4ae30cdd3772f8242

928 Newcastle University; University of East Anglia (2024): OpenCLIM: Catchment Discharges. NERC
929 EDS Centre for Environmental Data Analysis, *26 July 2024*. [Dataset]
930 doi:10.5285/a2e1601a29004c13849be5e84594f37a. https://dx.doi.org/10.5285/a2e160
931 1a29004c13849be5e84594f37a

932 NRFA (National River Flow Archive) [Dataset]. Available online:
933 https://nrfa.ceh.ac.uk/data/search. Accessed 1 Oct 2021

934 Olsson J, Lindström G (2008) Evaluation and calibration of operational hydrological ensemble
935 forecasts in Sweden. Journal of Hydrology 350:14–24.
936 https://doi.org/10.1016/j.jhydrol.2007.11.010

937 Otkin JA, Svoboda M, Hunt ED, et al (2018) Flash Droughts: A Review and Assessment of the
938 Challenges Imposed by Rapid-Onset Droughts in the United States.
939 https://doi.org/10.1175/BAMS-D-17-0149.1

940 Reyniers N, Osborn TJ, Addor N, Darch G (2023) Projected changes in droughts and extreme
941 droughts in Great Britain strongly influenced by the choice of drought index. Hydrology
942 and Earth System Sciences 27:1151–1171. https://doi.org/10.5194/hess-27-1151-2023

943 Robinson EL, Blyth EM, Clark DB, et al (2023) Climate hydrology and ecology research support
944 system potential evapotranspiration dataset for Great Britain (1961-2019) [CHESS-PE]

945 Smith BA, Birkinshaw SJ, Lewis E, et al (2024) Physically-based modelling of UK river flows under
946 climate change. Front Water 6:. https://doi.org/10.3389/frwa.2024.1468855

947 Sutanto SJ, Syaehuddin WA, de Graaf I (2024) Hydrological drought forecasts using precipitation
948 data depend on catchment properties and human activities. Commun Earth Environ
949 5:118. https://doi.org/10.1038/s43247-024-01295-w

950 Svensson C, Hannaford J, Prosdocimi I (2017) Statistical distributions for monthly aggregations
951 of precipitation and streamflow in drought indicator applications. Water Resources
952 Research 53:999–1018. https://doi.org/10.1002/2016WR019276

953 Swain DL, Prein AF, Abatzoglou JT, et al (2025) Hydroclimate volatility on a warming Earth. Nat
954 Rev Earth Environ 6:35–50. https://doi.org/10.1038/s43017-024-00624-z

955 Tan X, Wu X, Huang Z, et al (2023) Increasing global precipitation whiplash due to
956 anthropogenic greenhouse gas emissions. Nat Commun 14:2796.
957 https://doi.org/10.1038/s41467-023-38510-9

958 UK Government (2025) Drought declared in north-west of England. In: GOV.UK.
959 https://www.gov.uk/government/news/drought-declared-in-north-west-of-england.
960 Accessed 8 June 2025

961 UKCP18 Spatial files. [Dataset] Available online: https://ukclimateprojections-
962 ui.metoffice.gov.uk/help/spatial_files.

963 UKCP18-PET-BC. UKCP18-PET-and-Bias-Correction-for-Hydrology [Software]. Zenodo.
964 https://doi.org/10.5281/zenodo.17803787

965 van Pelt SC, Kabat P, ter Maat HW, Weerts AH (2009) Discharge simulations performed with a
966 hydrological model using bias corrected regional climate model input. Hydrol Earth Syst
967 Sci 13:2387–2397. https://doi.org/10.5194/hess-13-2387-2009

968 von Storch H, Zwiers F (2013) Testing ensembles of climate change scenarios for "statistical
969 significance." Climatic Change 117:1–9. https://doi.org/10.1007/s10584-012-0551-0

970 World Meteorological Organization (WMO) and Global Water Partnership (GWP) (2016)
971 Handbook of Drought Indicators and Indices (M. Svoboda and B.A. Fuchs). Integrated
972 Drought Management Programme (IDMP), Integrated Drought Management Tools and
973 Guidelines Series 2. Geneva

974 Zhang X, Alexander L, Hegerl GC, et al (2011) Indices for monitoring changes in extremes based
975 on daily temperature and precipitation data. WIREs Climate Change 2:851–870.
976 https://doi.org/10.1002/wcc.147

977 Zhang Y, Wang P, Chen Y, et al (2023) The optimal time-scale of Standardized Precipitation
978 Index for early identifying summer maize drought in the Huang-Huai-Hai region, China.
979 Journal of Hydrology: Regional Studies 46:101350.
980 https://doi.org/10.1016/j.ejrh.2023.101350

Expert Team on Climate Change Detection and Indices (ETCCDI). https://www.wcrp-climate.org/etccdi. Accessed 6 Aug 2025

References from the Supporting Information

Beven, K.J., Kirkby, M.J., 1979. A physically based, variable contributing area model of basin hydrology / Un modèle à base physique de zone d'appel variable de l'hydrologie du bassin versant. Hydrological Sciences Bulletin 24, 43–69. https://doi.org/10.1080/02626667909491834

Burnash, R.J.C., Ferral, R.L., McGuire, R.A., 1973. A Generalized Streamflow Simulation System: Conceptual Modeling for Digital Computers. U. S. Department of Commerce, National Weather Service, and State of California, Department of Water Resources.

Duan, Q., Sorooshian, S., Gupta, V.K., 1994. Optimal use of the SCE-UA global optimization method for calibrating watershed models. Journal of Hydrology 158, 265–284. https://doi.org/10.1016/0022-1694(94)90057-4

Kay, A.L., Davies, H.N., Lane, R.A., Rudd, A.C., Bell, V.A., 2021. Grid-based simulation of river flows in Northern Ireland: Model performance and future flow changes. Journal of Hydrology: Regional Studies 38, 100967. https://doi.org/10.1016/j.ejrh.2021.100967

Kingma, D.P., Ba, J., 2017. Adam: A Method for Stochastic Optimization. https://doi.org/10.48550/arXiv.1412.6980

Lane, R.A., Coxon, G., Freer, J.E., Wagener, T., Johnes, P.J., Bloomfield, J.P., Greene, S., Macleod, C.J.A., Reaney, S.M., 2019. Benchmarking the predictive capability of hydrological models for river flow and flood peak predictions across over 1000 catchments in Great Britain. Hydrology and Earth System Sciences 23, 4011–4032. https://doi.org/10.5194/hess-23-4011-2019

Leavesley, G.H., Lichty, R.W., Troutman, B.M., Saindon, L.G., 1983. Precipitation-runoff Modeling System: User's Manual (No. 83–4238). U.S. Geological Survey Water-Resources Investigations Report.

Lees, T., Buechel, M., Anderson, B., Slater, L., Reece, S., Coxon, G., Dadson, S.J., 2021. Benchmarking data-driven rainfall–runoff models in Great Britain: a comparison of long short-term memory (LSTM)-based models with four lumped conceptual models. Hydrology and Earth System Sciences 25, 5517–5534. https://doi.org/10.5194/hess-25-5517-2021

Liang, X., Lettenmaier, D.P., Wood, E.F., Burges, S.J., 1994. A simple hydrologically based model of land surface water and energy fluxes for general circulation models. Journal of

Geophysical Research: Atmospheres 99, 14415–14428. https://doi.org/10.1029/94JD00483

Nearing, G.S., Kratzert, F., Sampson, A.K., Pelissier, C.S., Klotz, D., Frame, J.M., Prieto, C., Gupta, H.V., 2021. What Role Does Hydrological Science Play in the Age of Machine Learning? Water Resources Research 57, e2020WR028091. https://doi.org/10.1029/2020WR028091

Smith, B.A., Birkinshaw, S.J., Lewis, E., McGrady, E., Sayers, P., 2024. Physically-based modelling of UK river flows under climate change. Front. Water 6. https://doi.org/10.3389/frwa.2024.1468855

Todini, E., 1996. The ARNO rainfall—runoff model. Journal of Hydrology 175, 339–382. https://doi.org/10.1016/S0022-1694(96)80016-3

Xu, T., Liang, F., 2021. Machine learning for hydrologic sciences: An introductory overview. WIREs Water 8, e1533. https://doi.org/10.1002/wat2.1533